ULTRA-SENSITIVE ON-CHIP GRAPHENE-BASED ELECTRO-OPTIC SENSOR ARRAYS FOR MULTIPLEXED NEURAL SIGNAL DETECTION

Xiang Li [*], *Zabir Ahmed* [*], *Harshvardhan Gupta, Kanika Sarna, Vishal Jain and Maysam Chamanzar*
Department of Electrical and Computer Engineering, Carnegie Mellon University, 5000 Forbes Avenue, Pittsburgh, PA 15213, USA

ABSTRACT

A novel graphene-integrated electro-optic nanophotonic sensor is demonstrated in this paper with very high sensitivity, capable of detecting sub-mV neural signals. The electrophysiological neural signals are detected by the graphene layer and encoded into the optical domain through interaction with an on-chip photonic micro resonator. This enables direct detection of neural signals without any optical tags such as calcium indicators. These sensors can be designed to operate at specific resonance wavelengths. Encoding the detected signals in the optical domain enables wavelength division multiplexing of neural recordings from multiple sensors over a single optical waveguide, thus enabling massive scaling of neural recording without having to dedicate one interconnect per channel to transmit the recorded neural signals. This will drastically minimize the size of the neural implant and will minimize brain tissue damage.

KEYWORDS

Neural Probes, Electro-optic Sensing, Optical Multiplexing, Integrated Photonics, Graphene

INTRODUCTION

Background

High throughput simultaneous neural recording from different areas of the brain with minimal level of invasiveness is necessary for a comprehensive understanding of neural circuits, which is critical for both advancing the frontiers of fundamental neuroscience research and also successful translation of research findings to clinical practice. However, a major bottleneck for large-scale neural recording is the trade-off between recording density and signal-to-noise ratio (SNR) [1].

Though substantial progress has been made over the past few decades in achieving large-scale neural recordings, the very high density of neurons in the brain necessitates a substantial increase in neural recording density to capture the intricacies of neural circuits. The neuronal density is several orders of magnitude higher than state-of-the-art neural probe channel density [2]. Traditional passive neural probes are based on a one-wire-per-channel scheme, where each electrode requires a dedicated interconnect wire to the backend amplifier, creating a size constraint for the probe. A higher channel density can be achieved using ultra-high-resolution lithography. However, increased channel crosstalk and signal attenuation, especially for long neural probes that reach deep regions of the brain limits the scalability of such neural probes. The introduction of complementary metal-oxide-semiconductor (CMOS)-based active probes has expanded the channel count to approximately a thousand channels on a single shank [3]. Yet, power consumption constraints in the active circuits impose limits to prevent tissue heating, and there are trade-offs involving noise and bandwidth in time domain multiplexing. In these architectures, only a subset of the channels on each probe shank can be simultaneously activated to capture neural signals. Still, tradeoffs between channel density and signal to noise ratio (SNR) for these neural probes limit the scalability.

Our solution

In this work, we discuss a novel electro-optic neural sensor that can detect and transduce the electrophysiological signals of neurons to a modulated optical signal. This sensor can address the scalability limitations of neural probes by leveraging wavelength-division multiplexing (WDM) of optical signals, which is widely used in optical communications [4]. WDM is a multiplexing technique that allows simultaneous transmission of multiple signals on a single optical fiber or on-chip waveguide, each at a specific wavelength. The transmitted signals can be demultiplexed and decoded at the receiver in the wavelength domain.

To utilize such optical multiplexing techniques for neural data transmission, the electrical neural signal first needs to be transduced to an optical signal. Given the variability of neural signals, which may range from tens of microvolts to several millivolts, we need an extremely sensitive transduction mechanism with a considerable dynamic range to convert the electrical signals into the optical domain. The device should record extracellular potentials and optically encode them without the need for exogenous contrast agents. In this work, we demonstrate a novel graphene-integrated electro-optic sensor capable of transducing sub-millivolt electrophysiological neural signals into the optical domain. When a neuron fires and generates and electrophysiological signal, the extracellular potential is detected by a graphene microelectrode situated on top of a photonic microresonator. The electric potential intercepted by the graphene layer is translated to a change of optical absorption in the monolayer graphene. This change of absorption modulates the optical response of the underlying photonic microresonator to encode the information in the neural signal into an optical signal.

In order to multiplex transduced electrical signals in the optical domain using different wavelengths, we utilize an array of microresonators to perform WDM on an integrated photonic chip as shown in Figure 1. Essentially, each of these microresonators operates at a particular resonance wavelength, which corresponds to a unique recording channel of the neural probe. A single optical waveguide (the bus waveguide) can be used to carry information from many of these microresonators, whose resonant wavelengths are slightly different from each other. We can passively multiplex information from multiple resonators via a single photonic waveguide by utilizing WDM. Therefore, this novel design obviates the need for routing multiple interconnect wires (i.e., one-wire-per-channel) as it is done in traditional passive neural probes.

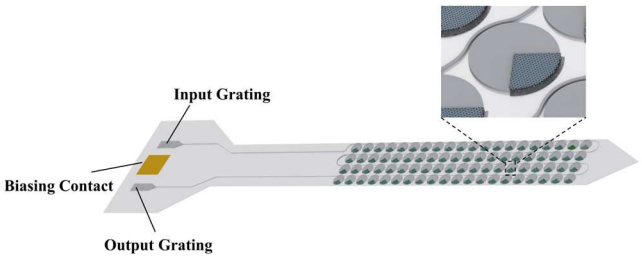

Figure 1: Design schematic of the optically multiplexed neural probe, featuring an array of electro-optic sensors. Each sensor unit includes a graphene-integrated micro resonator coupled to the shared bus waveguide. The electrophysiological signals are transduced into the optical domain at distinct wavelengths.

978-1-940470-05-4/HH2024/$25©2024TRF
DOI 10.31438/TRF.HH2024.5

WORKING PRINCIPLE

Electro-optic sensor

The main component of our system is a sensitive electro-optic sensor that integrates a graphene-based photonic microresonator coupled to an optical waveguide. The graphene covered silicon microresonator transduces electrophysiological signals into optical signals. When a neuron fires, the electric field in its vicinity experiences a rapid change due to the ion movement. Our electro-optic sensor leverages the unique properties of graphene to detect the small changes in the electric field in the medium. The optical absorption of graphene changes according to the applied electrostatic bias, since its Fermi level is modulated by the electrostatic bias, which can change continuously as the external electric field changes (Figure 2) [5].

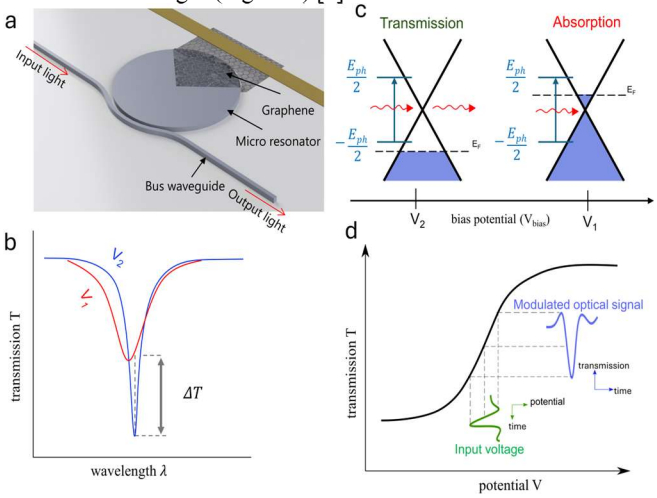

Figure 2: Working principle of graphene modulation. (a): Schematic of a unit cell of the electro-optic sensor, with different components labeled. (b): With different biasing potential, the Fermi level is modulated, which changes the optical transmission. (c): With different biasing potential, the transmission is shifted due to the absorption and phase modulation. (d): A schematic diagram shows the transduction of a small electrical signal to optical transmission modulation.

Although graphene's Fermi level can be tuned with an electrostatic bias, the total change in optical absorption due to a monolayer of graphene is still very small, and not sufficient for efficient electro-optic transduction of sub-millivolt electrical signals from neural tissue. To address this challenge, we integrate the monolayer graphene on a microresonator. The photonic microresonator is only partially covered with monolayer graphene. When light is coupled into the microresonator, it passes through the graphene-covered region multiple times, which effectively increases the interaction length. This enhancement is instrumental in addressing the issue of limited modulation of optical absorption in graphene layer.

The change of optical absorption in graphene changes the round-trip optical loss in the photonic microresonator, causing a change in its intrinsic quality factor Q_0. The change of the Q_0 induces a change of optical transmission through the coupled bus waveguide near the resonant wavelength of the microresonator. The transmission, T, through the waveguide, is related to the intrinsic quality factor, Q_0, and the resonance wavelength, λ_0, according to

$$T(\lambda, Q_0, Q_c) = \left| \frac{j2\lambda_0\left(\frac{1}{\lambda}-\frac{1}{\lambda_0}\right)+\frac{1}{Q_0}-\frac{1}{Q_c}}{j2\lambda_0\left(\frac{1}{\lambda}-\frac{1}{\lambda_0}\right)+\frac{1}{Q_0}+\frac{1}{Q_c}} \right|^2, \qquad (1)$$

where Q_c is the coupling quality factor, that is determined by the interaction length and gap between the bus waveguide and microresonator. When the operating wavelength, λ, is tuned near the resonance wavelength, λ_0, the change of external electrical field can induce a change of optical transmission, which can be detected by a photodetector. A small-amplitude time-varying input signal in the vicinity of the electro-optic sensor induces a proportional modulation of the optical transmission.

A highly sensitive sensor is critical for a high signal-noise ratio (SNR) of this device. We want the sensor to be sensitive enough to detect sub-millivolt electrophysiological signals in order to be used in a high-density sensor array. The gain of the electro-optic sensor can be defined as the ratio of relative change in the transmitted optical power through the bus waveguide (output) to the small amplitude neural signal (input), which can be calculated as

$$\frac{dT}{dV} = \frac{dE_F}{dV} * \frac{dQ_0}{dE_F} * \frac{dT}{dQ_0} \qquad (2)$$

Where T is the transmission, V is the neural signal voltage, E_F is the Fermi energy level, and Q_0 is the resonator intrinsic quality factor. The first term in the product relates the change in Fermi level to the applied electrostatic bias, which is determined by the capacitance at the interface of the monolayer graphene and the electrolyte, at the biasing potential. When we shift the biasing potential, the sensitivity of the Fermi level to the applied voltage shifts. An optimal biasing potential provides the highest sensitivity of Fermi level to the input voltage. The second term relates the intrinsic quality factor, Q_0, and the Fermi level, which corresponds to the interaction between graphene and the photonic microresonator. The graphene coverage area and the distance between graphene and the microresonator are the main factors that determine this interaction. The last term is a function of the coupling quality factor Q_C, which is controlled by engineering the coupling gap between the micro resonator and the bus waveguide.

Optical multiplexing

In the previous section, we have discussed how the electro-optic sensor can modulate electrical signals into optical signals at particular wavelengths. We can couple multiple electro-optic sensors of different dimensions, with different resonance wavelengths, to the same bus waveguide, that can transmit electrical signals from different channels at spectrally separated resonance wavelengths. Since these sensors are coupled to the same bus waveguide, we can multiplex the information at each channel through a single waveguide using WDM.

Fabrication

The complete fabrication process flow is shown in Figure 3. Our devices are fabricated on a silicon-on-insulator (SOI) chip with a 220 nm device layer and 2 µm of buried oxide. Electron-beam lithography (EBL) is used to pattern the photonic structures, including grating couplers, waveguides, and resonators. All the other patterns are created by contact photolithography. An inductively coupled plasma reactive ion etching (ICP RIE) shallow etching process defines the photonic devices by etching ~100 nm into the device silicon layer. Using a partial etch instead of a full silicon etch for the photonic devices can reduce scattering losses to improve the quality factors of the photonic resonators and minimizes the step height to reduce graphene tearing. The silicon outside of the photonic devices is fully etched in an additional ICP silicon etching process with a 3 µm ridge width. Then, a 7 nm layer of SiO_2 is deposited via the atomic layer deposition (ALD) process as the buffer layer between the silicon photonic microresonator and graphene. Afterwards, a monolayer of graphene covered with PMMA film is transferred onto the photonic devices using a wet

transfer process. After thermal annealing, the protective PMMA layer is removed in acetone at 65 °C for 30 minutes. The graphene film is patterned using photolithography and etching in oxygen plasma. A Ni-Au (10 nm/150 nm) layer is evaporated and patterned using a lift-off process to realize the biasing metal trace on the graphene. Finally, a 1.5 µm thick SU-8 layer is spin coated and patterned as the insulation layer. The photonic devices and biasing metal traces are insulated, while the graphene covered microresonators are exposed.

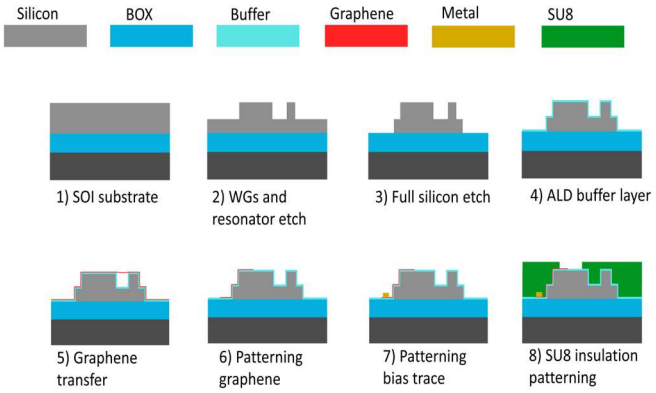

Figure 3: Fabrication process of graphene-integrated photonic microresonator.

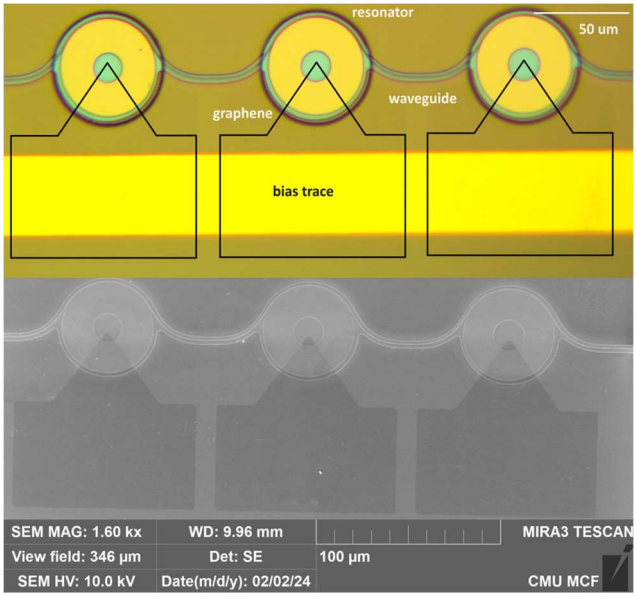

Figure 4: Fabricated device with sensor array of three resonators. The optical microscope image and SEM image. The SEM image is taken before metal deposition.

RESULT

Benchtop characterization

To validate the capability of individual sensors for recording sub-millivolt neural signals, we fabricated a sensor array consisting of three resonators with different resonance wavelengths as shown in Figure 4. The radius of each resonator is designed so that it operates at a distinct resonance wavelength. The outer radius is 25 µm, resulting in an FSR of ~4 nm. The coupling gap between the waveguide and the resonator is designed to achieve critical coupling.

A benchtop characterization of individual channels was conducted by placing the sensor in a phosphate buffered saline (PBS 1X) solution to mimic the electrochemical environment of neural tissue, as shown in Figure 5 (a). A tunable laser (Santec TSL-510), capable of operating in the range of 1500 nm to 1630 nm, provides optical input to the sensor during the benchtop characterization, and the optical response through the device is recorded using a photodetector. The biasing potential, provided by a signal generator, is increased from 0 mV to 600 mV in 50 mV steps. As shown in Figure 5 (b), the optical transmission centered around the resonance wavelength undergoes a dramatic change as the biasing potential is swept. The significant shift in optical transmission near the resonant wavelength validates the electro-optic modulation due to the change of electrical field near the graphene monolayer. As we can see from the figure, the electro-optic sensor gain varies as a function of the wavelength and biasing potential. There is an optimal operation point corresponding to the highest gain, which is used for the characterization of the small signal response of the device and for ex-vivo measurements.

We also measured the noise floor around the optimal operation point by applying a DC signal. Since the input signal only contains the DC component, all the AC power at the output corresponds to noise, allowing us to estimate the noise floor of individual channels. In addition to the biasing potential, small-amplitude sinusoidal electrical signals with different frequencies were applied to obtain the frequency response of the sensor. The noise level and frequency response as shown in Figure 5 (c) and (d), respectively, further validate the capability of the device to record neural signals, whose frequency content is usually below 10 kHz, with hundreds of microvolts amplitudes[6].

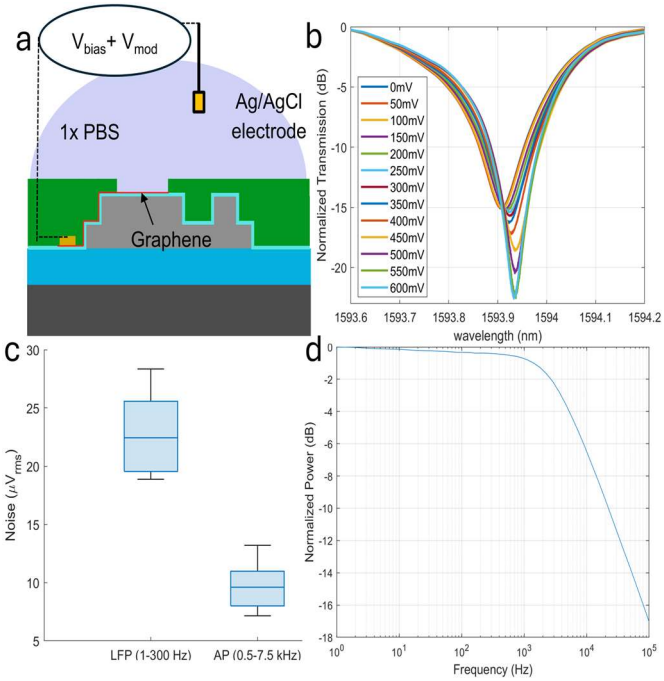

Figure 5: Benchtop characterization. (a): A schematic diagram illustrating the benchtop characterization. (b): Variation in the optical spectra of the electro-optic sensor with changes in biasing potential. (c): Input-referred noise of this channel. Two frequency bands are mainly considered in extracellular recording: local field potential band (1Hz -300 Hz) and action potential band (0.5kHz - 7.5 kHz). (d): Frequency response of the electro-optic sensor. The frequency response is flat enough for the frequency bands considered in extracellular recording.

Ex-vivo experiments

We have demonstrated that our electro-optic sensor can record electrical signals with sub-millivolt detection limit and high enough bandwidth to capture the temporal dynamics of neural signals very well. To validate that the electro-optic sensor can record actual biological neural signals, we conducted ex-vivo experiments with brain slices. The experiments were carried out by placing a 350 µm thick mouse brain slice on top of the electro-optic sensor in a perfused aCSF (artificial cerebrospinal fluid) environment. We applied biphasic electrical current stimulation to the slice and simultaneously monitored the evoked electrical response from the live neurons using our electro-optic sensor as well as a conventional neural recording system. A schematic of the arrangement is shown in Figure 6 (a).

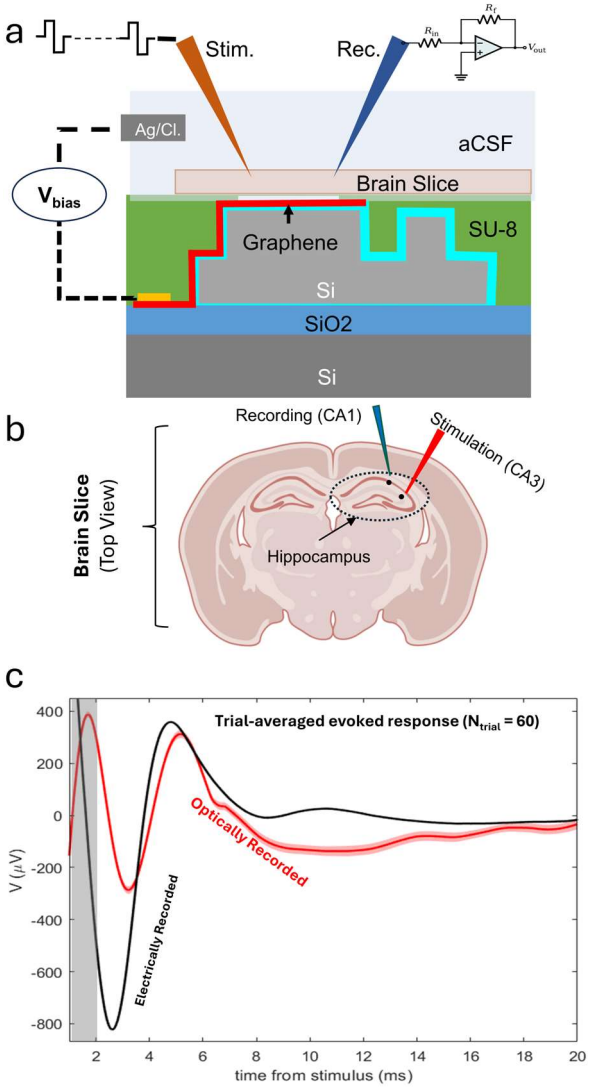

Figure 6: ex-vivo experiments to validate capability of neural recording. (a): A schematic diagram illustrating the ex-vivo experiment setup. (b): Diagram depicting the positioning of the brain slice over the electro-optic sensor. (c): Comparison between simultaneous electrical recordings and optical recordings from the same location. The averaged response from the brain slice is the solid line, and the standard error is the shadow. Both recordings consist of 60 trials. The amplitude and shape difference can be attributed to differences in the shape, area, and positioning of the electrode and the electro-optic sensor.

Biphasic electrical current stimulation was applied to the CA3 region of the hippocampus using a Pt-Ir bipolar concentric electrode connected to a neuro stimulator (Ripple Grapevine), while the electro-optic sensor was positioned underneath the CA1 region. We placed the tungsten monopolar electrode at the same location (CA1) to perform simultaneous electrical recording using a conventional neural recording system (Intan) and compared it with the optical recording to validate our device. The arrangement of the stimulation and recording electrodes is shown in Figure 6 (b).

We can observe a good match between the neural response recorded by the tungsten electrode and the electro-optic sensor, as shown in Figure 6 (c). This match validates that our electro-optic sensor can indeed record neural signals. Furthermore, our device can perform wavelength division multiplexing with appropriate design.

CONCLUSION

The graphene-integrated electro-optic neural sensor discussed in this paper can record sub-millivolt neural signals. The demonstrated sensor is designed to be sensitive enough to detect and transduce neural signals into an optically modulated signal. Our preliminary results show the possibility of using such electro-optic sensors in a wavelength division multiplexing scheme for a truly parallel multiplexed neural recording with the potential for massive scaling of neural recording.

ACKNOWLEDGEMENTS

This material is based upon work supported in part by the National Science Foundation under Grant No. 1926804. The authors acknowledge the use of the Bertucci Nanotechnology Laboratory at Carnegie Mellon University supported by grant BNL-78657879. The authors also acknowledge the use of the Materials Characterization Facility at Carnegie Mellon University supported by grant MCF-677785.

REFERENCES

[1] A. E. Urai, B. Doiron, A. M. Leifer, and A. K. Churchland, "Large-scale neural recordings call for new insights to link brain and behavior," *Nature Neuroscience*, vol. 25, no. 1. 2022. doi: 10.1038/s41593-021-00980-9.

[2] A. Nurmikko, "Challenges for Large-Scale Cortical Interfaces," *Neuron*, vol. 108, no. 2. 2020. doi: 10.1016/j.neuron.2020.10.015.

[3] J. J. Jun *et al.*, "Fully integrated silicon probes for high-density recording of neural activity," *Nature*, 2017, doi: 10.1038/nature24636.

[4] S. N. Khonina, N. L. Kazanskiy, M. A. Butt, and S. V. Karpeev, "Optical multiplexing techniques and their marriage for on-chip and optical fiber communication: a review," *Opto-Electronic Advances*. 2022. doi: 10.29026/oea.2022.210127.

[5] M. Liu *et al.*, "A graphene-based broadband optical modulator," *Nature*, vol. 474, no. 7349, 2011, doi: 10.1038/nature10067.

[6] M. Zhang, Z. Tang, X. Liu, and J. Van der Spiegel, "Electronic neural interfaces," *Nature Electronics*, vol. 3, no. 4. 2020. doi: 10.1038/s41928-020-0390-3.